Journal of Crystal Growth 51 (1981) 273–278

SOLID STATE MORPHOLOGICAL INSTABILITY OF Ni_4Mo PRECIPITATES

L.A. NESBIT
IBM, Burlington, Essex Junction, Vermont 05452, USA

and

D.E. LAUGHLIN
Metallurgy and Materials Science Department, Carnegie-Mellon University, Pittsburgh, Pennsylvania 15213, USA

Received 27 May 1980

The morphology of ordered Ni_4Mo precipitates in an off-stoichiometric Ni–Ni_4Mo alloy is documented at relatively high aging temperatures (low supersaturation) and compared to the precipitate morphology at low to intermediate aging temperature (large supersaturation). It is found that the precipitate morphology is a function of the aging temperature. In particular, at low aging temperatures the precipitates develop into ellipsoids with a square cross-section. At high temperatures, the precipitates appear to be subject to morphological instabilities normally associated with liquid-to-solid transformations. Consequently, the observed precipitates tend to form solid-state dendritic protrusions at the high aging temperatures.

1. Introduction

The morphology of ordered Ni_4Mo precipitates in an off-stoichometric Ni–Ni_4Mo alloy is a function of the degree of supersaturation at which the alloy is isothermally aged. Previous work [1] has shown that when at low to intermediate temperature (700 to 750°C), the Ni_4Mo precipitates in such an alloy develop into the shape of ellipsoids. The major diameter of the ellipsoid lies along the c-axis of the ordered Ni_4Mo (D1a, body-centered tetragonal) structure, and the geometry of the precipitates as observed along the c-axis is that of a square. Fig. 1 shows a schematic diagram of the precipitate shape at these temperatures. In fig. 1, the direction and Miller indices are given both with respect to the disordered fcc structure (subscript α) and with respect to the ordered D1a structure (subscript β). The direction and Miller indices used throughout the remainder of the paper are given with respect to the fcc structure.

The purpose of this paper is to document the various stages of the precipitate morphology at a higher aging temperature, where the formation of the Ni_4Mo precipitate is not as copious, and individual precipitates may grow relatively unimpeded by surrounding precipitates.

2. Experimental procedures

The composition of the off-stoichiometric alloy is Ni–16.7wt%Mo and its preparation is discussed elsewhere [1]. Sheet specimens were homogenized at 1000°C (1273 K) for approximately one hour prior to down-quenching to 775°C (1048 K) for various aging times up to 13,000 min. This aging temperature represents an undercooling of 60°C below the two-phase solvus temperature for this alloy.

Thin foils of the aged specimens were prepared by the twin-jet technique in a solution of 1/3 nitric acid and 2/3 methanol, cooled at −25°C (248 K). The foils were then examined with a JEM 100B transmission electron microscope, operating at 100 kV.

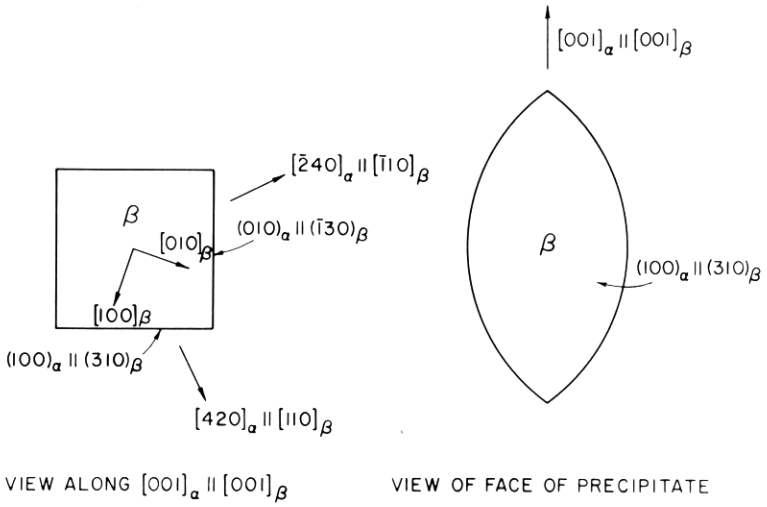

Fig. 1. The Ni_4Mo precipitate morphology after aging at 700°C for 1000 min. (a) View along the $[001]_\alpha \parallel [001]_\beta$ direction. (b) View of the precipitate face.

3. Results

At the relatively high aging temperature of 775°C, the ordered Ni_4Mo precipitates nucleate both heterogeneously on dislocations and on grain boundaries [2] and also, apparently, homogeneously within the supersaturated solid solution matrix. When nucleation is homogeneous, the precipitates initially have a morphology similar to that of precipitates formed at lower aging temperatures. If the precipitates experience unhindered growth, "spikes" develop in the $\pm[110]$ and $\pm[1\bar{1}0]$ direction. Both of the above growth stages are shown in fig. 2, in which the letter "A" designates a small precipitate shortly after nucleation and the letter "B" marks a precipitate that has undergone additional growth and consequently spikes have developed in the $\langle 110 \rangle$ directions. The viewing direction for both precipitates is along the D1a *c*-axis.

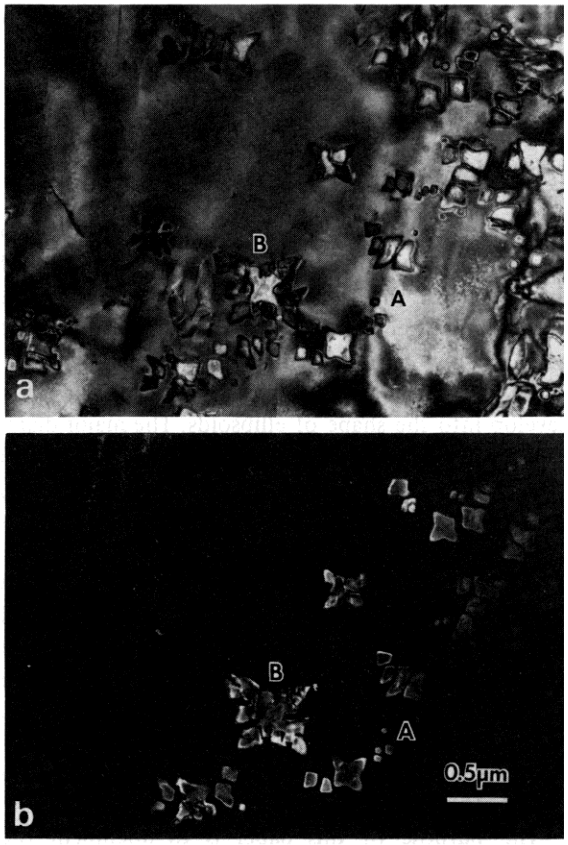

Fig. 2. The Ni–Mo alloy aged at 775°C for 1000 min as observed along the $[001]_\alpha$ zone axis. (a) Bright-field micrograph taken under multiple-beam diffracting conditions. (b) Dark-field micrograph of nearly the same area produced by imaging only one superlattice reflection. See the text for the significance of the letters "A" and "B".

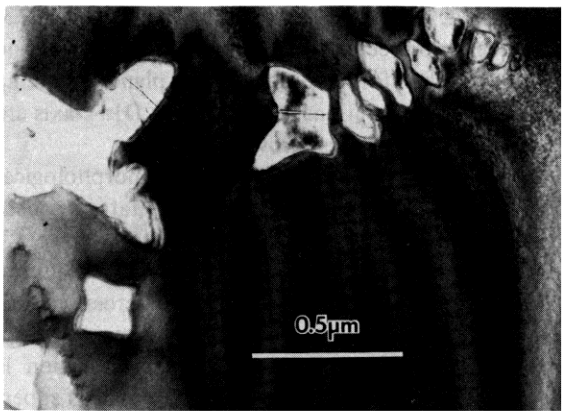

Fig. 3. The Ni–Mo alloy aged at 775°C for 1000 min. The precipitates to the upper right of the micrograph are all of the same orientation variant and are aligned in approximately the $[110]_\alpha$ direction. $\boldsymbol{n} = [001]_\alpha$.

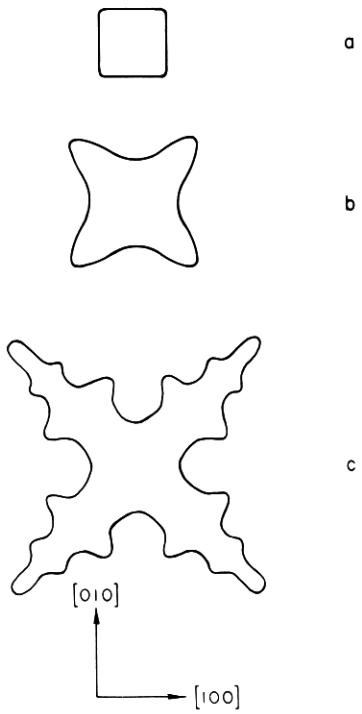

Fig. 4. Schematic drawings of the Ni_4Mo precipitate morphology at various aging times at 775°C. The direction of observation is from along the D1a c-axis. (a) Short aging times. (b) Intermediate aging times. (c) Long aging times.

As the spikes continue to grow, additional or secondary ⟨110⟩ protrusions develop from the original or primary spikes, as illustrated in fig. 3. The spacing of these secondary protrusions is on the order of several tens of nanometers. A schematic drawing of the Ni_4Mo precipitates at various stages of growth, as observed along the D1a c-axis, is shown in fig. 4.

Another interesting feature of the precipitate morphology at 775°C is that precipitates, with their c-axes in a common fcc cube direction, often appear in groups. In such instances, one large precipitate may have several smaller precipitates surrounding it or adjacent to it (fig. 2). In addition, when any two such precipitates are reasonably close together, the adja-

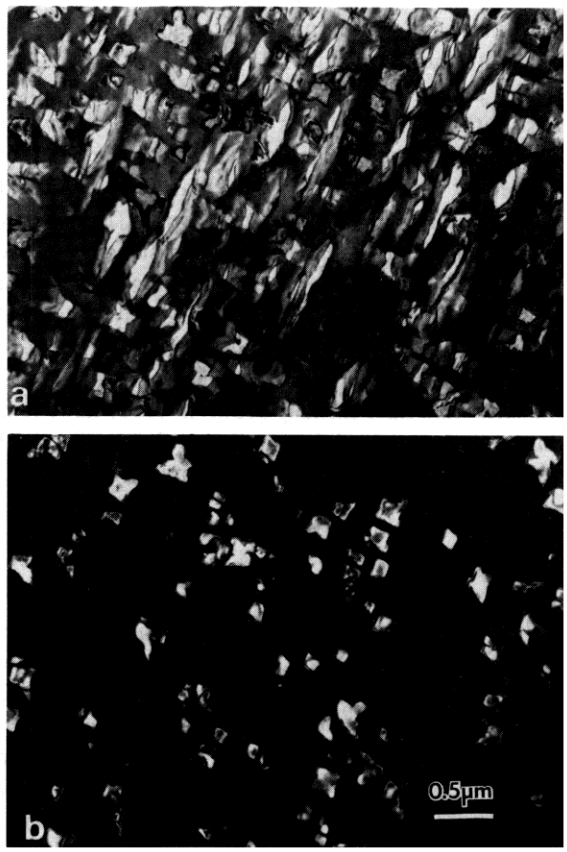

Fig. 5. The Ni–Mo alloy aged at 775°C for 600 min. (a) Bright field micrograph taken under multiple-beam diffracting conditions near $\boldsymbol{n} = [001]_\alpha$. (b) Dark-field micrograph of the same area as (a) produced by imaging both superlattice reflections on the (001) diffraction pattern.

cent facets of the precipitates lie along parallel {100} planes.

An indication as to why the precipitates appear to form in clusters is provided by a comparison of figs. 5a and 5b. This pair of electron micrographs shows the alloy microstructure as observed along the [001] direction in both bright- and dark-field. This dark-field micrograph is obtained by imaging both of the superlattice reflections on the (001) diffraction pattern. Thus all of the precipitates with their c-axes parallel to the [001] direction are imaged in the dark-field micrograph (fig. 5b). The remaining precipitates which are observed in the bright-field micrograph (but not in the dark-field micrograph) have their c-axes perpendicular to the [001] direction and parallel to either the [100] or the [010] directions. These latter precipitates are two to four times longer than they are wide, and their long dimension lies parallel to their particular D1a c-axis direction.

The important feature of concern with regard to these latter precipitates is that a few of the wider precipitates are branched-out into two projections parallel to the c-axis. This observation implies that the clustered precipitates (e.g. shown in fig. 2) may not have nucleated individually, but instead may have grown from a common parent precipitate. It should also be noted that precipitates in a given cluster will often be arranged in a ⟨110⟩ direction with respect to each other, as shown in fig. 3. This suggests that the branches may have initially grown in ⟨110⟩ directions from the parent precipitate, prior to their subsequent growth in the perpendicular ⟨001⟩ direction.

4. Discussion

The previous investigation [1] of the Ni_4Mo precipitate morphology at lower aging temperature demonstrated that the direction of easiest growth is along the D1a c-axis of the precipitate, which is also the direction of minimum strain (see fig. 1). If the growth of individual precipitates is uninhibited by either structural heterogeneities or by other precipitates, as is the case when annealed at 775°C, then it becomes apparent that the directions of easy growth in the plane normal to the precipitate c-axis are the $\pm[110]$ and $\pm[1\bar{1}0]$ directions. These directions of easy growth are evidenced by primary protrusions or spikes in the ⟨110⟩ direction as shown in figs. 2 and 3. Whenever two precipitates are reasonably close to one another, facets form on the {100} planes, evincing that the ⟨100⟩ directions normal to the D1a c-axis are the directions of slowest growth.

Chernov [3,4] has analyzed the morphological transition of a two-dimensional precipitate proceeding from the shape of a square (fig. 4a) to a "skeletal" shape (fig. 4b). For a constant flux of solute diffusing toward a growing particle with a square cross-section, the supersaturation is not constant at all points on its surface or interface. Instead the supersaturation is greater at the corners than at the faces. This supersaturation inhomogeneity becomes even more pronounced as the precipitate continues to grow, and eventually it results in the square cross-section becoming unstable and forming spikes in the direction of greatest supersaturation (and greatest growth rate). The particular size at which this instability occurs in dependent upon the degree of supersaturation inhomogeneity, the mass transport properties of the system, and the degree of anisotropy of the precipitate's growth rate. The approximate size at which the square cross-section becomes unstable at 775°C (1048 K) in the Ni–Mo alloy under investigation is 90 to 120 nm (see fig. 3).

In addition to the primary spikes in the ⟨110⟩ directions which develop at 775°C, small secondary perturbations develop on the primary spikes themselves and grow in perpendicular ⟨1$\bar{1}$0⟩ directions. These secondary protrusions appear to form and grow as the primary spike is growing, so that protrusions farther away from the tip of the primary spike are larger (have a greater amplitude) than those closer to the tip. As viewed from along the c-axis of a precipitate, the primary spikes are similar to solidification dendrites growing in the ⟨110⟩ directions, with secondary dendrites emanating from behind the tip of the primary dendrite. See fig. 3. These secondary perturbations are manifestations of a second type of solid state morphological instability which takes place at the interface between the precipitate and the surrounding matrix. This type of instability was first analyzed from a dynamic or kinetic point of view by Mullins and Sekerka [5] for the case of a solid particle undergoing diffusion-controlled growth in a liquid matrix.

In order to determine whether or not these sec-

ondary protrusions may be the result of such a morphological instability, it is informative to measure the radius of a spike where a small secondary protrusion (small in amplitude) has begun to develop and then to use this value to calculate certain pertinent physical parameters, and ascertain if such calculated values are physically reasonable. The parameters which will ultimately be evaluated are the Gibbs–Thompson coefficient, Γ, the critical radius of nucleation, R^*, and the precipitate–matrix interfacial energy, σ.

In their formulation, Mullins and Sekerka [5] consider the diffusion-controlled growth of a nearly spherical particle from a supersaturated solid solution with an initial uniform solute concentration of c_∞. The critical radius of nucleation is then given by the equation

$$R^* = 2\Gamma/[(c_\infty - c_0)/c_0] \,, \tag{1}$$

where c_0 is the concentration of the matrix at the precipitate–matrix interface. For diffusion-controlled growth, c_0 is the concentration of the matrix in equilibrium with the precipitate. For this particular alloy at 775°C, $c_\infty = 0.168$ and $c_0 = 0.150$ so that eq. (1) becomes

$$R^* = 16.7\Gamma \,. \tag{2}$$

Mullins and Sekerka then subject the spherical particle to an infinitesimal shape distortion by a single spherical harmonic, characterized by the letter l. For a given value of l, the average wavelength between nodes of the harmonic is expressed as $\lambda = 2\pi R/l$, where R is the radius of the particle. For a precipitate of Ni_4Mo, which has four-fold symmetry about its c-axis, Sekerka [6] has suggested using a value of $l = 4$ in subsequent calculations.

Assuming a *critical shape* rather than a *critical radius* as the criterion for instability, eq. (13) of Mullins and Sekerka [5] is employed as the stability/instability criterion:

$$\frac{\delta/\dot{\delta}}{R/\dot{R}} = (l-1)\left[1 - \frac{R_c(l)}{R}\right]\left[1 - \frac{R^*}{R}\right]^{-1} . \tag{3}$$

In this equation δ is the amplitude of the perturbation and $\dot{\delta} = \mathrm{d}\delta/\mathrm{d}t$ is the rate of growth of this amplitude. As already stated, R is the radius of the precipitate and $\dot{R} = \mathrm{d}R/\mathrm{d}t$. $R_c(l)$ is given by the equation

$$R_c(l) = [\tfrac{1}{2}(l+1)(l+2) + 1]\, R^* . \tag{4}$$

A shape instability occurs when $(\delta/\dot{\delta})/(R/\dot{R}) > 1$. Using a value of $l = 4$ and combining eqs. (2) and (4) into eq. (3) yields

$$\frac{\delta/\dot{\delta}}{R/\dot{R}} = 3\left[\frac{R - 267.2\Gamma}{R - 16.7\Gamma}\right] \tag{5}$$

The sides of the primary ⟨110⟩ spikes, similar to those in fig. 3, may be viewed as having a radius R. The radii of several such spikes were measured which had very small secondary protrusions and were found to have an average value of $R = 160$ nm. This value may be taken as the critical radius for a shape instability and substituted for R in eq. (5). When eq. (5) is set equal to one, Γ is calculated as 0.41 nm. Substituting $\Gamma = 0.41$ nm into eq. (2) gives a critical radius of nucleation 6.8 nm. Although this value of R^* may seem large, it is not unreasonable for this particular alloy considering the relatively small supersaturation it experiences at 775°C. (The radius of the smallest observable precipitate in fig. 2 is about 7.0 nm.)

Another parameter of interest which may be calculated from the above results is the precipitate/matrix interfacial energy σ, as given by rearranging eq. (22.34) of Christian [7]:

$$\sigma = \frac{\Gamma k T}{v^\beta}\,\frac{x^\beta - x^\alpha}{1 - x^\alpha} \,, \tag{6}$$

where v^β is the atomic volume of the β or precipitate phase, k is Boltzmann's constant, x^α is the composition of the matrix in equilbrium with the precipitate of composition x^β. For the Ni–Ni_4Mo system at 775°C (1048 K), $x^\alpha = 0.15$, $x^\beta = 0.20$, and the atomic volume of the ordered Ni_4Mo phase is 0.0117 nm^3/atom. These values yield an interfacial energy of 30 erg/cm^2, which compares favorably with the free energy of a twin boundary in Ni at 1060°C (1333 K) of 43 erg/cm^2 [8] and with the interfacial energy of a γ' precipitate in a Ni–Al alloy of 18.5 erg/cm^2 [9].

Since reasonable values of Γ, R^*, and σ have been calculated based upon the Mullins and Sekerka formulation of morphological instability, the secondary perturbations along the primary ⟨110⟩ spikes may justifiably be considered solid state morphological instabilities or solid state dendrites.

As the primary ⟨110⟩ spikes grow at 775°C, they eventually reach a region sufficiently distant from the main body of the precipitate that growth is once

again most favorable parallel to the *c*-axis ([001] direction) of the precipitate. This growth sequence (⟨110⟩ spike, followed by growth in the [001] direction) would explain why some precipitates branch into two or more projections along the D1a *c*-axis (fig. 5a) and also why adjacent precipitates often have *c*-axes in identical ⟨100⟩ directions (figs. 2 and 3). Adjacent precipitates with the same D1a *c*-axis may be branches or fingers emanating from a common parent precipitate.

In summary, the overall view of the precipitate morphology and the factors controlling it in the Ni–Ni_4Mo system are as follows. The direction of easiest growth is along the D1a *c*-axis, which is also the direction of minimum strain. As a result the precipitates have the shape of ellipsoids at low to intermediate aging temperatures and shortly after they nucleate at 775°C. As the precipitates grow, they form facets on the {100} planes, parallel to the D1a *c*-axis, These facets are probably the result of anisotropic growth rates, which are a maximum in those ⟨110⟩ directions, which are in the plane normal to the D1a *c*-axis. If the precipitates form copiously throughout the matrix, their diffusion fields soon overlap and the precipitates retain their square cross-section normal to their *c*-axis throughout the aging process. If, instead, the precipitates grow unimpeded by surrounding precipitates and/or their diffusion fields, then primary protrusions develop in the ⟨110⟩ directions. From these primary protrusions, secondary perturbations develop, which are manifestations of a solid state morphological instability and may be thought of as solid state dendrites. Finally, growth may also take place parallel to the precipitate *c*-axis from primary protrusions resulting in the apparent formation of clusters of precipitates as viewed along their common D1a *c*-axis.

Acknowledgements

We would like to thank Dr. S.R. Coriell and Professor R.F. Sekerka for helpful discussions during the course of this work. This research was sponsored by the National Science Foundation, Division of Materials Research, Grant No. DMR-7805723.

References

[1] L.A. Nesbit and D.E. Laughlin, Acta Met. 26 (1978) 815.
[2] L.A. Nesbit, Ph.D. Thesis, Carnegie–Mellon University (1978).
[3] A.A. Chernov, J. Crystal Growth 24/25 (1974) 11.
[4] A.A. Chernov, in: Crystal Growth and Characterization (Proc. of the ISSCG2, Springschool, Japan, 1974), Eds. R. Ueda and J.B. Mullin (North-Holland, Amsterdam, (1975).
[5] W.W. Mullins and R.F. Sekerka, J. Appl. Phys. 34 (1963) 323.
[6] R.F. Sekerka, private communications to D.E. Laughlin and L.A. Nesbit.
[7] J.W. Christian, The Theory of Transformations in Metals and Alloys, 2nd ed. (Pergamon, Oxford, 1975).
[8] L.E. Murr, Scripta Met. 6 (1972) 203.
[9] R.G. Faulkner and B. Ralph, Acta Met. 20 (1972) 703.